A spectral model for unidirectional nonlinear wave propagation over arbitrary depths

S. Beji [a], K. Nadaoka [b,*]

[a] *Department of Naval Architecture and Ocean Engineering, Istanbul Technical University, Maslak 80626, Istanbul, Turkey*
[b] *Graduate School of Information Science and Engineering, Tokyo Institute of Technology, 2-12-1 O-okayama, Meguro-ku, Tokyo 152, Japan*

Abstract

A weakly-nonlinear and dispersive wave equation recently developed by the authors is used for formulating a spectral-type unidirectional wave propagation model describing spectral transformations of narrow-band waves travelling over arbitrary depths. The essential characteristics of the model equation are recapitulated first and then the spectral domain representation in terms of spatially varying harmonic amplitudes is presented. The resulting evolution equations are used to simulate the experiments concerning harmonic generation in shallow water and nonlinear random wave transformations over a submerged bar. Furthermore, the spectral model predictions are compared with the field measurements in nearshore with satisfactory results. © 1999 Elsevier Science B.V. All rights reserved.

Keywords: Spectral model; Nonlinear random waves; Shallow water waves; Deep water waves; Harmonic generation; Spectral transformations

1. Introduction

Nearshore zone is characterized by highly nonlinear wave motions that manifest themselves as asymmetric and skewed wave profiles, and ultimately breaking. While accurate representations of such complicated motions are still beyond the reach of the

---

* Corresponding author. Tel.: +81-3-75734-2589; Fax: +81-3-75734-2650; E-mail: nadaoka@mei.titech.ac.jp

present state-of-the-art, substantial progress has been made over the last two decades in unravelling various facets of the nonlinear phenomenon.

A penetrating account of the nonlinear shoaling waves was given by Freilich and Guza (1984) who proposed two wave models as variants of the Boussinesq equations and presented the corresponding spectral domain formulations along with comparisons with the field measurements. The success of the Boussinesq-type equations in simulating the nonlinear shallow water wave transformations stimulated the attempts to extend their applicable domain so as to cover large enough areas for practical applications (Witting, 1984; Madsen et al., 1991; Madsen and Sørensen, 1992; Nwogu, 1993; Beji and Nadaoka, 1996a). For varying bathymetry Mase and Kirby (1992) proposed a hybrid model, which was a modified form of the spectral domain representation of the KdV equation. Madsen and Sørensen (1993) used their improved Boussinesq equations for producing spectral models for constant and varying depths and investigated the higher-order boundary conditions. Agnon et al. (1993) formulated a weakly-nonlinear, fully-dispersive unidirectional spectral model based on the standard equations of potential theory for surface waves.

In order to overcome the depth restrictions associated with Boussinesq models, Nadaoka et al. (1994, 1997) derived a set of fully-dispersive, nonlinear wave equations modelling the evolution of broad-band directional wave fields over arbitrary depths. The special forms of these general equations were manipulated further, resulting in two new wave models describing transformations of narrow-band directional and unidirectional nonlinear waves (Beji and Nadaoka, 1997a). All these wave equations are formulated in time domain via a new approach named *multi-term coupling technique* and therefore they differ considerably from the unidirectional spectral model of Agnon et al. (1993).

The present work employs the unidirectional wave model of Beji and Nadaoka (1997a) which is not restricted to only shallow or only deep waters but is operational in the entire range of relative depths. In shallow water the equation simulates the conoidal and solitary waves while in deep water it admits the second-order Stokes waves as solution. When the incident wave frequency coincides with the prescribed dominant frequency of the wave model the linear shoaling rate of the incident wave is predicted exactly, in perfect agreement with the energy flux concept.

The outline of the paper is as follows. In Section 2, the linear dispersion, linear shoaling, and nonlinear properties of the wave model are examined. In Section 3 the surface displacement is represented as a Fourier series with spatially varying amplitudes and phases, and a set of nonlinearly coupled first-order differential equations describing the spatial variations of each harmonic amplitude is obtained. Section 4 contains the numerical simulations using the evolution equations derived in Section 3 for the experiments of Chapalain et al. (1992) on harmonic generation in shallow water and for nonlinear random wave transformations over a submerged bar (Beji and Battjes, 1993). Furthermore, the field measurements in nearshore zone (Nakamura and Katoh, 1992), covering a distance of nearly 2 km, are compared with the computations with quite acceptable results. Finally, for extending the applicability of the model to the surf zone, the possibility of including wave breaking effects in a heuristic manner as a simple dissipation term (Mase and Kirby, 1992; Battjes et al., 1993; Beji and Nadaoka, 1997b) is pointed out.

2. General characteristics of wave model

The wave equation used in this work (Beji and Nadaoka, 1997a) is

$$
C_g \eta_t + \frac{1}{2} C_p (C_p + C_g) \eta_x - \frac{(C_p - C_g)}{k^2} \eta_{xxt} - \frac{C_p(C_p - C_g)}{2k^2} \eta_{xxx}
$$
$$
+ \frac{1}{2} \left[C_p(C_g)_x + (C_p - C_g)(C_p)_x \right] \eta + \frac{3}{4} g \left(3 - 2\frac{C_g}{C_p} - \frac{k^2 C_p^4}{g^2} \right) (\eta^2)_x = 0,
$$

(1)

where C_p, C_g, and k are respectively the phase and group velocities and the wave-number computed according to the linear theory dispersion relation for a dominant wave frequency ω and a given local depth h, the subscripts x and t indicate partial differentiation with respect to space and time, respectively.

For very shallow water waves $C_p = C_g = \sqrt{gh}$ and Eq. (1) reduces to the combined unidirectional form of Airy's nonlinear non-dispersive equations. If the lowest-order dispersion is retained by letting $C_p = \sqrt{gh}\,(1 - k^2 h^2/6)$ and $C_g = \sqrt{gh}\,(1 - k^2 h^2/2)$ then a straightforward manipulation of Eq. (1) leads to the KdV equation. Furthermore, for infinitely deep water waves the model equation admits the second-order Stokes waves as solution. Thus, Eq. (1) may be interpreted as a unified nonlinear wave model describing evolution of a narrow-band wave field from infinitely deep to very shallow waters with smooth transition.

2.1. Linear dispersion characteristics

The linear dispersion characteristics of the wave model may be investigated by assuming an incident wave of the form $\eta = a \exp i(\Omega t - Kx)$, substituting it into the linearized, constant depth form of Eq. (1), and then solving for Ω/K which represents the phase celerity of the wave form as dictated by the wave model. After normalizing the phase celerity $C = \Omega/K$ by the shallow water wave speed $\sqrt{gh}$, one gets

$$
\frac{C}{\sqrt{gh}} = \frac{1}{2} \sqrt{\frac{\tanh kh}{kh} \left[\frac{(1+r) + (1-r)\xi^2}{r + (1-r)\xi^2} \right]},
$$

(2)

in which $r = C_g/C_p = (1/2)(1 + 2kh/\sinh 2kh)$, and $\xi = K/k$ is the ratio of the incident arbitrary wave-number to the specified wave-number of the model equation.

According to linear theory the exact expression for wave celerity C_e for an arbitrary wave number K is given by

$$
\frac{C_e}{\sqrt{gh}} = \sqrt{\frac{\tanh \xi kh}{\xi kh}}.
$$

(3)

For a selected $(h/L)^*$ ratio (L: wavelength) the corresponding kh and r values may be computed, and then by varying $\xi = K/k = Kh/kh = (h/L)/(h/L)^*$ in the neighbourhood of the fixed $(h/L)^*$, the approximate and exact phase celerities may be computed for a range of arbitrary (h/L) values. Fig. 1 compares Eqs. (2) and (3) for
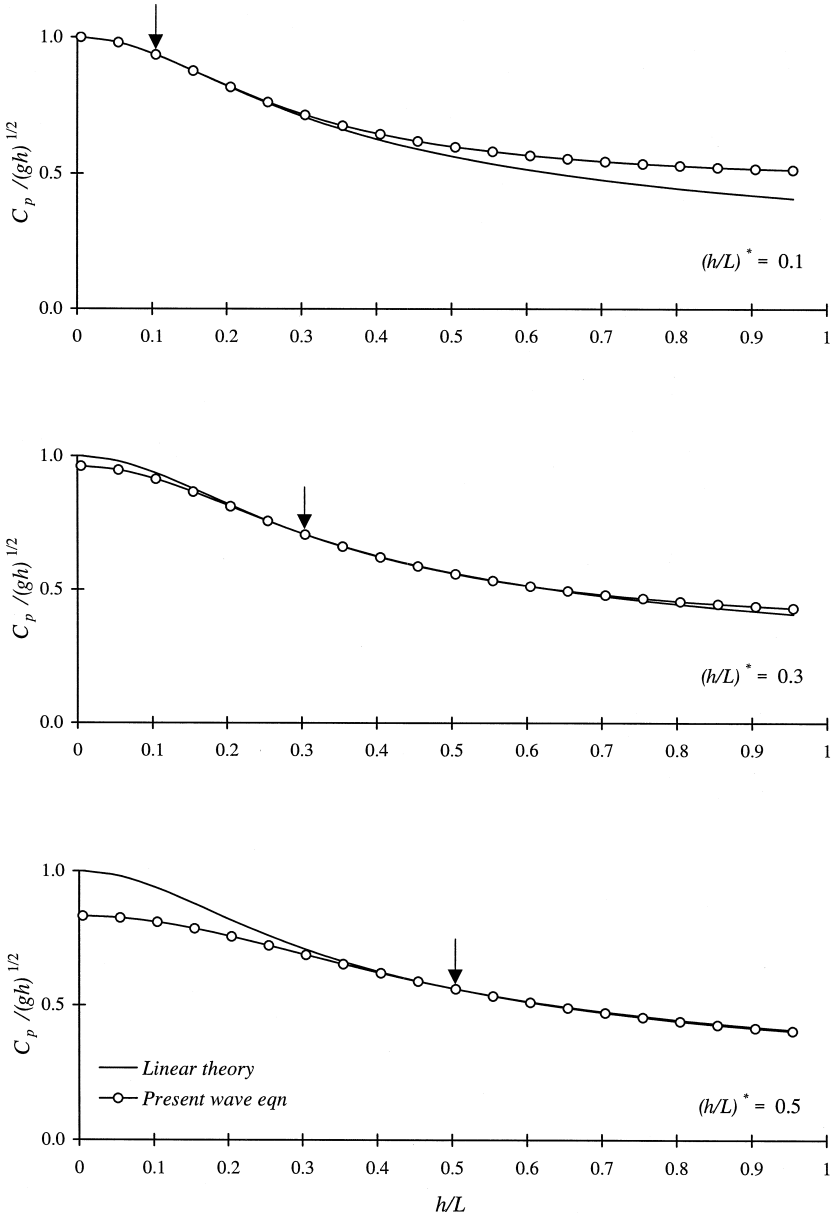
Fig. 1. Comparisons of linear theory phase speed and the phase speed of the present wave model for three different specifications of the model parameters which correspond to shallow $(h/L)^* = 0.1$, intermediate $(h/L)^* = 0.3$, and deep $(h/L)^* = 0.5$ water waves.

three different selected $(h/L)^*$ values. When the arbitrary (h/L) value is the same as the selected $(h/L)^*$; that is $\xi = 1$, $C = C_e$ hence there is no error. In the close neighbourhood, for $1/2 < \xi < 3/2$, C is virtually inseparable from C_e and the accuracy

is quite high. Only for relatively large deviations of ξ from unity the errors become sensible but not unacceptable.

2.2. Linear shoaling characteristics

An important aspect in modelling wave transformations over variable sea bed is the linear shoaling characteristics of the wave model employed. The standard Boussinesq equations with the effects of variable depth incorporated predict the linear shoaling with less than 1% error if $(h/L) < 0.06$ while the alternative form of the Boussinesq equations do better and satisfy the same criterion for $(h/L) < 0.3$, as reported by Nwogu (1993). Beji and Nadaoka (1996a) give a similar result for their improved Boussinesq equations.

The present model does not suffer from any inherent depth restriction; if the incident wave frequency coincides with the prescribed wave frequency of the model the linear shoaling rate is predicted exactly for any relative depth. This point may be easily demonstrated using the approach introduced by Madsen and Sørensen (1992). An incident wave of the form $\eta = a(x)\exp[\omega t - \int k(x)\mathrm{d}x]$ is substituted into the wave equation and the higher derivatives of $a(x)$ and $k(x)$ are neglected so that an expression for the spatial variation of $a(x)$ is obtained. Carrying out this procedure for Eq. (1) results in $a_x/a = -(C_g)_x/2C_g$, which is the same as the expression given by linear theory.

If the incident wave frequency and wave-number are taken to be arbitrary, as in Section 2.1, then deviations from the exact linear shoaling rate in the neighbourhood of the specified model frequency and wave-number may be investigated. As outlined in the preceding paragraph, the procedure may be carried out in a straightforward manner; however, the expressions are lengthy and therefore no detail is given here. Fig. 2 compares the variations of the linear shoaling coefficient α (that is, for $a_x/a = -\alpha h_x/h$, see Madsen and Sørensen, 1992 for details) of the wave model and of the linear theory for three different cases which correspond to respectively shallow, intermediate, and deep water specifications of the model equation parameters. In each case, when the incident wave parameters and the model equation parameters are identical the linear shoaling coefficients become identical as well, indicating that the wave model predicts the linear shoaling rate exactly. Deviations from the theory in the vicinity of $(h/L)^*$ are more appreciable compared to those in Fig. 1 because the shoaling characteristics of a wave model are dictated by expressions an order higher than those of the dispersion characteristics.

2.3. Solitary waves

The solitary wave represents a balance between nonlinearity and dispersion. As long as C_p is not exactly equal to C_g, Eq. (1) contains both dispersion and nonlinearity, which implies that it must admit a permanent wave of the solitary type as an analytical solution. Thus, we seek a solution of the form

$$\eta = H\cosh^{-2}\left[(x - C_s t)/l_s\right], \tag{4}$$

where H is the prescribed wave height, l_s and C_s are respectively the length scale and the phase speed of the solitary wave which are yet unknown constants to be determined

from the wave equation. Substituting Eq. (4) into Eq. (1) and solving for l_s and C_s so that Eq. (4) satisfies Eq. (1) exactly, we obtain

$$l_s = \sqrt{\frac{3(C_p - C_g)\left(C_p^2 + \frac{4}{3}\beta H\right)}{\beta k^2 C_g H}} \ , \quad C_s = \frac{C_p(C_p + C_g)}{2C_g} + \frac{2\beta H}{3C_g}, \qquad (5)$$

where $\beta = \frac{3}{4}g(3 - 2C_g/C_p - k^2 C_p^4/g^2)$ is the coefficient of the nonlinear term in Eq. (1). A matter of historic concern is immediately evident from the form of l_s. It becomes zero when $C_p = C_g$; that is, purely nondispersive waves cannot maintain a permanent form simply because there exists no dispersivity to counterbalance the steepening action of nonlinearity. However, allowing the lowest-order dispersion by approximating $C_p \simeq \sqrt{gh}(1 - k^2 h^2/6)$ and $C_g \simeq \sqrt{gh}(1 - k^2 h^2/2)$, as in the Boussinesq theory, is sufficient to obtain a permanent form. If these approximate forms are used in Eq. (5) and the higher-order dispersion contributions are dropped,

$$l_s \simeq \sqrt{\frac{4h^3(1 + H/h)}{3H}} \ , \quad C_s \simeq \sqrt{gh}\left(1 + \frac{1}{2}\frac{H}{h}\right), \qquad (6)$$

which are in complete agreement with the classical expressions (see for instance Miles, 1980). In particular, it is interesting to note that l_s is the same as the Rayleigh (1876) result and for small H/h it may be approximated as $\sqrt{4h^3/3H}$, which is the well-known expression.

2.4. Stokes waves

As for the solitary waves, we shall assume that the wave Eq. (1) is capable of producing the second-order Stokes waves:

$$\eta = a\cos(\kappa x - \omega t) + b\cos 2(\kappa x - \omega t), \qquad (7)$$

in which a and ω are the prescribed primary wave amplitude and frequency, κ and b are to be determined from the wave model. Substituting Eq. (7) into Eq. (1) and collecting the zeroth- and first-order terms result in

$$\kappa = k, \quad b = \frac{\beta}{3C_p(C_p - C_g)}a^2, \qquad (8)$$

where the interaction of the primary wave with the second-harmonic is excluded in the above analysis to be consistent with the second-order perturbation approach. It must be indicated that, unlike a truncated perturbation solution, the present wave model, being an evolution equation, always produces a nonlinear dispersion effect which makes κ different from the linear theory wave number k (see Beji and Nadaoka, 1996b).

According to the Stokes theory the amplitude of the second-harmonic for an arbitrary relative depth (Wiegel, 1964, p. 29) is

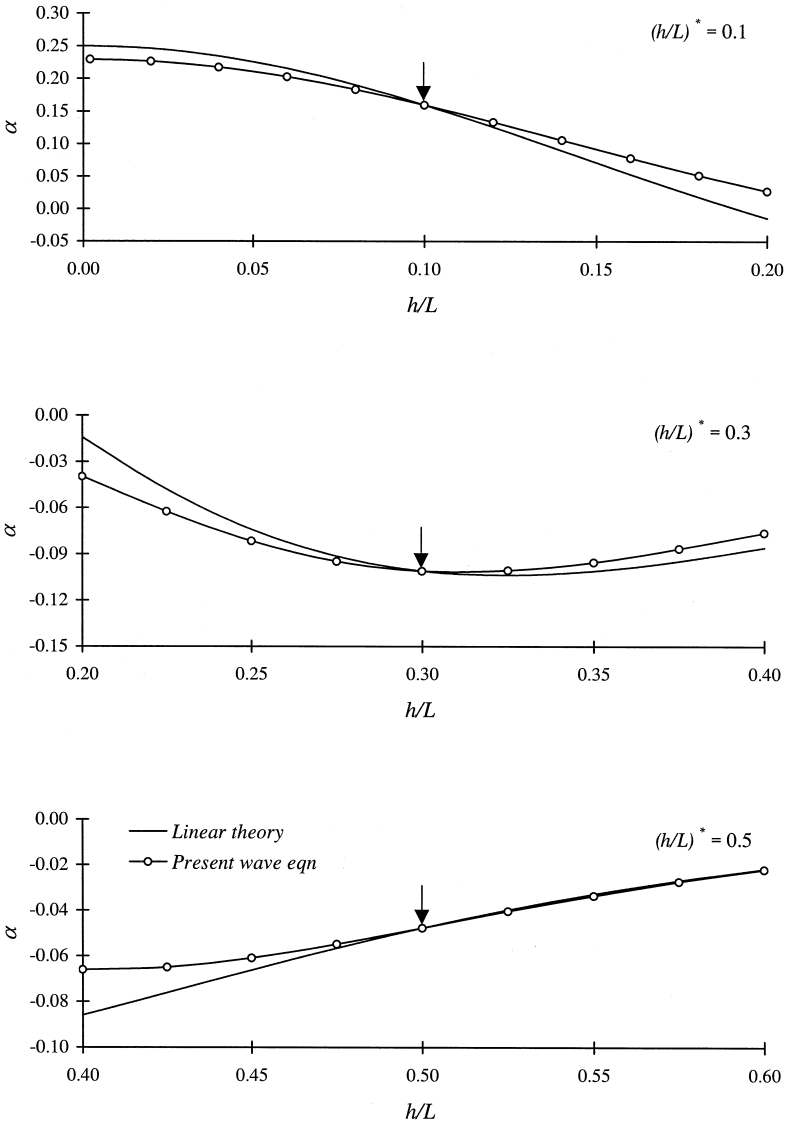$$b_s = \frac{1}{2}ka^2\frac{\cosh kh\left(1 + \frac{1}{2}\cosh 2kh\right)}{\sinh^3 kh}. \qquad (9)$$

Fig. 2. Variations of the coefficient of the linear shoaling gradient α (for $a_x / a = -\alpha h_x / h$) according to linear theory and the present wave equation for shallow $(h/L)^* = 0.1$, intermediate $(h/L)^* = 0.3$, and deep $(h/L)^* = 0.5$ water specifications of the model parameters.

Considering the deep water waves, $C_p = \sqrt{g/k}$, $C_g = C_p/2$, and $\beta = \frac{3}{4}g$. Thus, comparing Eq. (8) with Eq. (9), $b = b_s = \frac{1}{2}ka^2$, which is the same as the second-order theory predicts. For relatively intermediate and shallow depths b differs from b_s at most by 7%, as is shown in Fig. 3, where the difference percentage, $100(b_s - b)/b_s$, is depicted for a wide range of relative depths. Since the Stokes theory
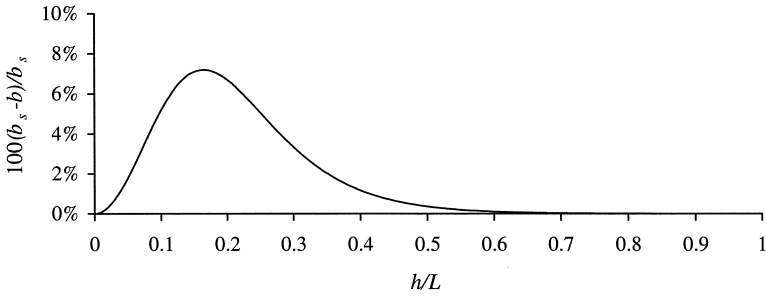
Fig. 3. Percentage of difference between b_s (Stokes theory) and b (present wave model), $100(b_s - b)/b_s$, for a wide range of relative depths.

is reliable only for small Ursell numbers (see Mei, 1989, p. 620) the lower h/L range in Fig. 3 should be viewed with caution.

3. Evolution equations

A set of evolution equations describing the spatial changes of the component wave amplitudes of a prescribed incident wave field propagating over arbitrary water depths is now derived. A Fourier series representation of the surface displacement with spatially varying amplitudes and phases is assumed:

$$\eta(x,t) = \sum_{n=-\infty}^{+\infty} A_n(x) e^{i[\omega_n t - \int k_n(x)\mathrm{d}x]}, \tag{10}$$

where $i = \sqrt{-1}$, $A_n(x)$ is the spatially varying complex wave amplitude, ω_n is the radian frequency which is equal to $n\Delta\omega$, $\Delta\omega$ being the frequency of resolution. $k_n(x)$ is the spatially varying wave-number determined according to the linear dispersion relation of Eq. (1) for the local depth $h(x)$ and the radian frequency ω_n:

$$C_g \omega_n - \frac{1}{2} C_p(C_p + C_g) k_n + \frac{(C_p - C_g)}{k^2} \omega_n k_n^2 - \frac{C_p(C_p - C_g)}{2k^2} k_n^3 = 0. \tag{11}$$

Substituting Eq. (10) into Eq. (1) and neglecting the third-order derivatives of $A_n(x)$, on the premise that the spatial variations of $A_n(x)$ is slow, result in the following second-order nonlinear differential equation that determines the spatial variation of each complex component:

$$i\alpha_2 \frac{\mathrm{d}^2 A_n}{\mathrm{d}x^2} + \alpha_1 \frac{\mathrm{d}A_n}{\mathrm{d}x} + (\alpha_s + i\alpha_0) A_n$$

$$= i\beta \sum_{m=-\infty}^{+\infty} (k_m + k_{n-m}) A_m A_{n-m} e^{-i(k_m + k_{n-m} - k_n)x}, \tag{12}$$

where free index n covers the range from $-\infty$ to $+\infty$. The spatial derivatives of $k_n(x)$ higher than the first have been neglected in accordance with the model Eq. (1). The coefficient of the nonlinear terms, β, has already been defined; the rest of the coefficients are

$$\alpha_0 = C_g \omega_n - \frac{1}{2} C_p (C_p + C_g) k_n + \frac{(C_p - C_g)}{k^2} \omega_n k_n^2 - \frac{C_p (C_p - C_g)}{2 k^2} k_n^3$$

$$\alpha_1 = \frac{1}{2} C_p (C_p + C_g) - 2 \frac{(C_p - C_g)}{k^2} \omega_n k_n + \frac{3 C_p (C_p - C_g)}{2 k^2} k_n^2$$

$$\alpha_2 = \frac{(C_p - C_g)}{k^2} \left(\frac{3}{2} C_p k_n - \omega_n \right)$$

$$\alpha_s = \frac{1}{2} \left[C_p (C_g)_x + (C_p - C_g)(C_p)_x \right] + \frac{(C_p - C_g)}{k^2} \left(\frac{3}{2} C_p k_n - \omega_n \right) (k_n)_x, \tag{13}$$

in which $(k_n)_x$ is computed from Eq. (11) by differentiating it with respect to x. Note that α_0 is the linear dispersion relation of the wave model and is identically zero in virtue of Eq. (11). However, if the wave numbers in Eq. (10) are selected as bound wave numbers then α_0 is not zero any more and it must be retained in Eq. (12). In principle, the wavenumbers may be chosen either way, here they are selected as free wave numbers according to Eq. (11), which numerically proved to be a better choice except in the simulation of the Stokes second-order waves.

The linear shoaling coefficient α_s is a function of the bed slope and therefore $\alpha_s A_n$ may be considered a slowly varying contribution, just like the nonlinear term $A_m A_{n-m}$. Then, by assuming $\alpha_s A_n$ and $A_m A_{n-m}$ locally constant, an analytical integration with respect to x becomes possible. Following Bryant (1973) we multiply Eq. (12) by $-i/\alpha_2 \exp(-i \alpha_1/\alpha_2 x)$ so that it may be re-written as

$$\frac{d}{dx} \left(\frac{d A_n}{dx} e^{-i \alpha_1 x/\alpha_2} \right) = i \frac{\alpha_s}{\alpha_2} A_n e^{-i \alpha_1/\alpha_2 x} + \beta \sum_{m=-\infty}^{+\infty} \frac{(k_m + k_{n-m})}{\alpha_2}$$

$$\times A_m A_{n-m} e^{-i(k_m + k_{n-m} - k_n + \alpha_1/\alpha_2)x}, \tag{14}$$

in which α_0 has been set to zero. Ignoring the spatial variations of $\alpha_s A_n$ and $A_m A_{n-m}$ and integrating with respect to x result in

$$\frac{d A_n}{dx} = -\frac{\alpha_s}{\alpha_1} A_n$$

$$+ i \beta \sum_{m=-\infty}^{+\infty} \left[\frac{k_m + k_{n-m}}{\alpha_1 + \alpha_2 (k_m + k_{n-m} - k_n)} \right] A_m A_{n-m} e^{-i(k_m + k_{n-m} - k_n)x}. \tag{15}$$

Eq. (15) in its present form is not suitable for numerical treatment and should be manipulated further. The summations are first re-arranged to run in the positive range only. Then, $A_n(x)$ is set to $\frac{1}{2}[a_n(x) - ib_n(x)]$ so that the evolution equations for the real variables $a_n(x)$ and $b_n(x)$ are obtained

$$
\begin{aligned}
\frac{\mathrm{d}a_n}{\mathrm{d}x} = &- \frac{\alpha_s}{\alpha_1}a_n \\
&+ \beta \sum_{m=1}^{N-n} \alpha^+ \left[(a_m b_{n+m} - a_{n+m}b_m)\cos\theta^+ + (a_m a_{n+m} + b_m b_{n+m})\sin\theta^+ \right] \\
&+ \frac{1}{2}\beta \sum_{m=1}^{n-1} \alpha^- \left[(a_m b_{n-m} + a_{n-m}b_m)\cos\theta^- + (a_m a_{n-m} - b_m b_{n-m})\sin\theta^- \right]
\end{aligned}
$$
(16)

$$
\begin{aligned}
\frac{\mathrm{d}b_n}{\mathrm{d}x} = &- \frac{\alpha_s}{\alpha_1}b_n \\
&- \beta \sum_{m=1}^{N-n} \alpha^+ \left[(a_m a_{n+m} + b_m b_{n+m})\cos\theta^+ - (a_m b_{n+m} - a_{n+m}b_m)\sin\theta^+ \right] \\
&- \frac{1}{2}\beta \sum_{m=1}^{n-1} \alpha^- \left[(a_m a_{n-m} - b_m b_{n-m})\cos\theta^- - (a_m b_{n-m} + a_{n-m}b_m)\sin\theta^- \right]
\end{aligned}
$$
(17)

where N is the number of frequency components retained in the solution, and

$$
\alpha^+ = \frac{k_{n+m} - k_m}{\alpha_1 + \alpha_2 \delta^+}, \qquad \alpha^- = \frac{k_{n-m} + k_m}{\alpha_1 + \alpha_2 \delta^-},
$$

$$
\delta^+ = k_{n+m} - k_m - k_n, \qquad \delta^- = k_{n-m} + k_m - k_n,
$$

$$
\theta^+ = \int_0^x (k_{n+m} - k_m - k_n)\mathrm{d}x, \qquad \theta^- = \int_0^x (k_{n-m} + k_m - k_n)\mathrm{d}x.
$$
(18)

It should be remarked that the linear shoaling characteristics of the original equation are preserved in the above formulation. The free index n runs from 1 to N, resulting in $2N$ number of nonlinearly coupled first-order differential equations for the unknown components $a_n(x)$ and $b_n(x)$. Once the $a_n(x)$ and $b_n(x)$ are obtained the free surface may be constructed from Eq. (10). Various numerical integration techniques (e.g., Adams–Bashford–Moulton, Bulirsch–Stoer, Runge–Kutta) are available for the integration of Eqs. (16) and (17). Here, the Runge–Kutta fourth-order formulation is preferred as it proved to be the fastest while being as reliable as the others.

An alternative formulation is possible via a change of variable $A_n(x) = P_n(x)\exp(i\int k_n dx)$ which removes the sine and cosine functions as in Bryant (1973). The resulting evolution equations are simpler but their numerical integration requires smaller spatial steps (e.g., usually 1/5 of the step required for the above equations) and therefore the computational efficiency is questionable.

4. Numerical simulations

The evolution equations derived in Section 3 are now used for the purposes of ascertaining their reliability and exploring the capabilities of the wave model.

4.1. Harmonic generation in shallow water

Chapalain et al. (1992) conducted a series of experiments concerning nonlinear shallow water waves undergoing harmonic generation over constant water depth. The experiments were done for four different cases named respectively as the trial A, C, D, and H. The experimental conditions and wave parameters are given in Table 1.

All the experiments listed in Table 1 are numerically simulated using the evolution equations derived in Section 3. In the computations six harmonic components $\omega_n = n\omega_0$, $n = 1, \ldots, 6$ were used with ω_0 denoting the primary wave frequency. Fig. 4 shows the measured and computed harmonic components for the first four harmonics for the trials A, C, D, and H. Overall, the numerical simulations appear to be in good agreement with the measurements. The beat lengths are slightly underestimated; this is probably due to the limitation of the wave model to relatively narrow-band cases. Since the third and fourth harmonics fall outside the narrow-band range of the primary wave the restriction is somewhat violated.

4.2. Nonlinear wave evolutions over a submerged bar

Nonlinear transformations of random waves travelling over a submerged bar were investigated by Beji and Battjes (1993) in laboratory experiments that revealed the relative importance of the effects shaping the wave spectrum. The waves were first observed to undergo harmonic generation due to nonlinear interactions in the shoaling region and then the bound harmonics were released as the water depth increased in the lee side of the bar. For relatively long waves an initially single-peaked spectrum was observed to transform to a double-peaked spectrum. Due to the absence of near-resonant interactions, the short wave evolutions were not substantial.

The experimental measurements for random waves initially having a JONSWAP type wave spectrum with peak frequencies of $f_p = 0.5$ Hz (long waves) and $f_p = 0.8$ Hz (short waves) are simulated using Eqs. (16) and (17). For each case, the dominant frequency for the model equation was set to the mean frequency of the incident spectrum. The records of the surface elevation at Station 1 were divided into 10 segments of 2048 data points and then each segment was Fourier transformed. Out of

Table 1

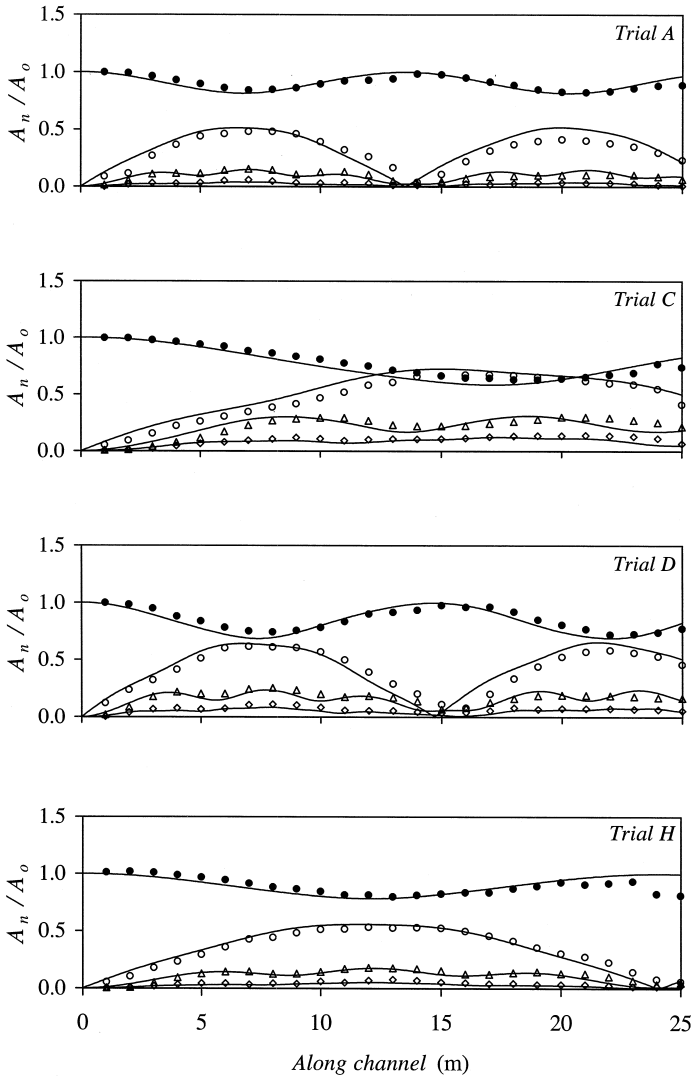| Trial	h (cm)	T (s)	$\varepsilon = a_0 / h$	$\mu = kh$	$U_r = \varepsilon / \mu^2$
A	40	2.5	0.105	0.528	0.38
C	40	3.5	0.105	0.371	0.76
D	30	2.5	0.118	0.452	0.58
H	40	3.0	0.084	0.433	0.45

Fig. 4. Experimental data on harmonic generation in shallow water (Chapalain et al., 1992) compared with the computations for the trials A, C, D, and H for the first four harmonics. Scatter: experiment, solid line: computation.

the 1024 unique pairs the first 325 Fourier components, which covered a frequency range of 0.0125–4.0 Hz, were found to be quite sufficient to represent the incident wave spectrum hence the spectral model was run for 10 different realizations with $\Delta \omega = 2 \pi \times 0.0125$ rd/s and $N = 325$, using the measured Fourier components as the incoming boundary condition at Station 1.

Fig. 5 shows the comparisons for measured and computed spectra at three selected stations for the long and short wave cases. The spectra were obtained after ensemble
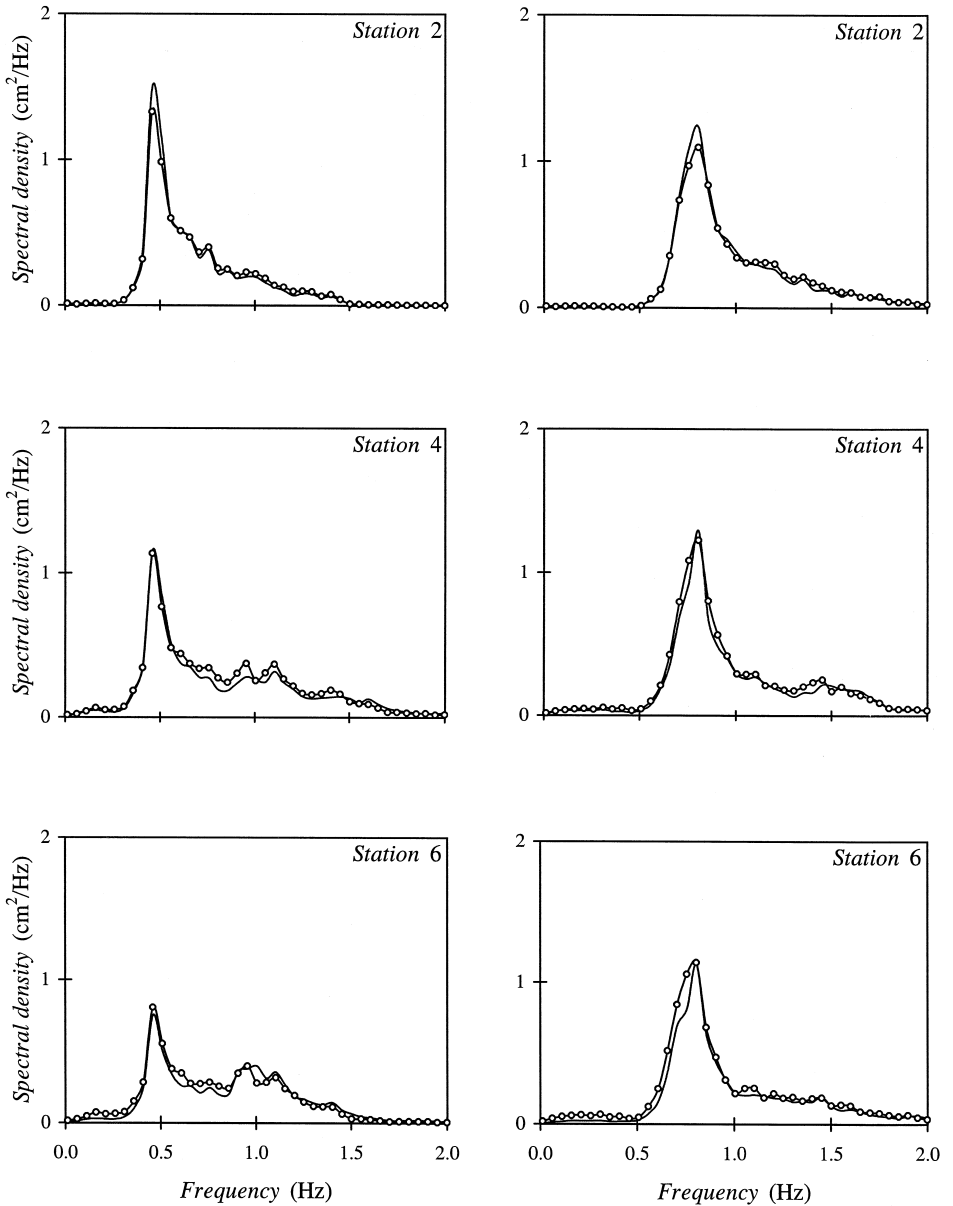
Fig. 5. Comparisons of the experimental measurements of nonlinear random wave propagation over a submerged bar with the numerical simulations. Left column: Long-wave evolutions ($f_p = 0.5$ Hz). Right column: Short-wave evolutions ($f_p = 0.8$ Hz). Station 2: upslope 1:20, water depth 0.16 m; Station 4: horizontal bottom, water depth 0.1 m; Station 6: downslope 1:10, water depth 0.3 m.

averaging all the realizations and frequency smoothing five neighbouring components. Each spectrum then has 100 degrees of freedom and 14% normalized standard error. The
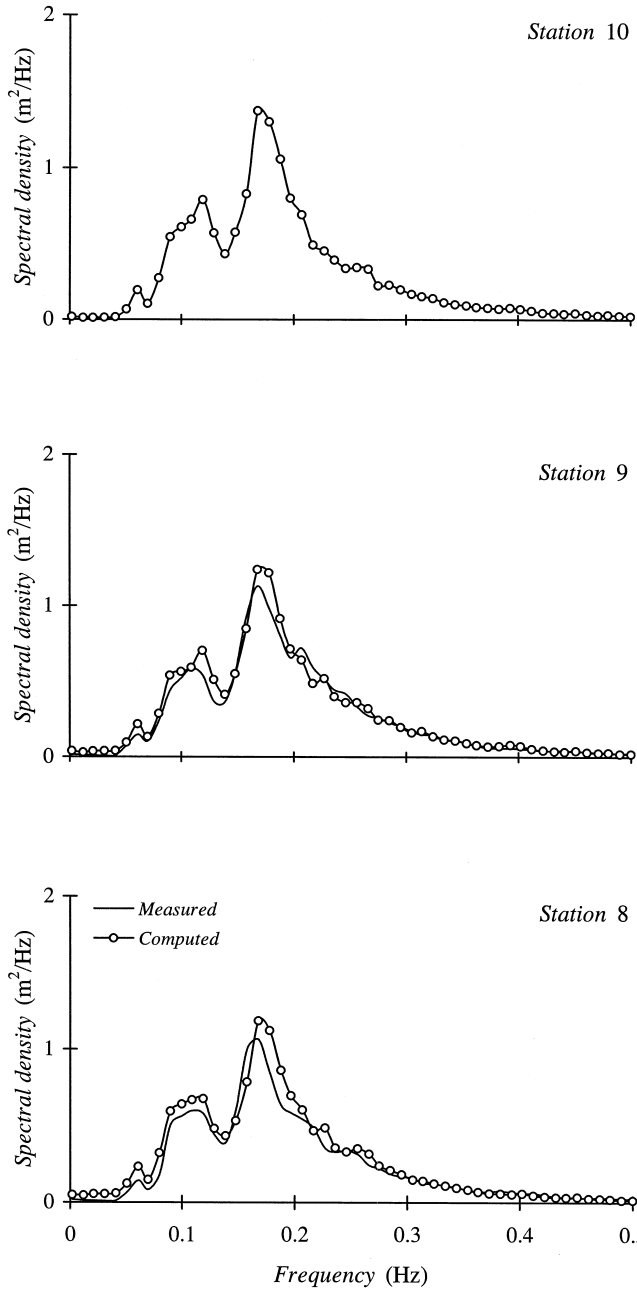
Fig. 6. Comparisons of the field measurements of Nakamura and Katoh (1992) with the numerical simulations for incident waves with mean wave height 1.8 m and mean frequency 0.2 Hz. Station 10: Incident boundary, 3200 m from the shoreline, water depth 24 m; Station 9: 2100 m from the shoreline, water depth 14 m; Station 8: 1300 m from the shoreline, water depth 9 m.

agreement of the computations with the both sets of measurements is remarkably good, and small discrepancies are attributed to the inherently narrow-banded nature of the wave model, which gives rise to errors in computed wavenumbers well outside the neighbourhood of the dominant wave wavenumber.

4.3. Waves in nearshore zone

Nakamura and Katoh (1992) carried out field measurements from 25 February 1989 to 1 March 1989 at the Hazaki Oceanographical Research Facility (HORF) near Kashima, Japan. The site of the field observations is a natural sandy beach facing the Pacific Ocean. Ten ultrasonic wave gauges were used, of which seven were installed on the 427 m-long observatory pier while the remaining three were deployed at water depths of 9 m (Station 8), 14 m (Station 9), and 24 m (Station 10), located respectively at distances of 1.3, 2.1, and 3.2 km from the shoreline. Data was continuously sampled at a rate of 2 Hz for 2-h durations, at 6-h time intervals. A quantitative assessment made by Nwogu et al. (1992) using the maximum entropy method provides convincing evidence that for practical purposes the wave field in this particular region may be considered unidirectional.

Since the first seven measurement stations were located in the surf zone the majority of the waves were breaking and the wave model in its present form could not be used. Therefore, only the nearshore Stations 8, 9, and 10 were considered; the measured data at Station 10 served as the incoming boundary condition. Comparisons were made for the data of February 25, which represents a typical sea state with a peak frequency of $f_p = 0.175$ Hz and mean wave height 1.8 m.

The collected data at Station 10 was segmented into 12 groups of 1024 data points and Fourier transformed. Of the 512 unique transformed pairs, the first 360 components which covered a frequency range between 0.002 to 0.7 Hz were considered sufficient to represent the incident spectrum. The dominant frequency of the wave model was set to the peak frequency of the incident wave spectrum and the computations were performed for 12 different realizations with $\Delta \omega = 2 \pi \times 0.002$ rd/s and $N = 360$. Fig. 6 shows the measured and computed spectra at Stations 10, 9, and 8. Each spectrum has 192 degrees of freedom and 10% normalized standard error. The agreement is quite reasonable, especially if allowances are made for the uncertainties involved in the unidirectionality of waves and the exact form of the bottom topography.

5. Concluding remarks

A spectral model based on a weakly-nonlinear unidirectional wave equation is developed. The resulting evolution equations describe the nonlinear transformations of narrow band wave fields over arbitrary depths with acceptable accuracy. The performance of the spectral model for non-breaking waves appears to be reliable, as evidenced by the comparisons with the experimental and field measurements. To extend its applicable domain to the surf zone, where the effects of breaking waves must be taken into account, a semi-empirical approach in the form of a dissipation term may be adopted as in Beji and Nadaoka (1997b).

Acknowledgements

References

Agnon, Y., Sheremet, A., Gonsalves, J., Stiassnie, M., 1993. Nonlinear evolution of a unidirectional shoaling wave field. Coastal Eng. 20, 29–58.

Battjes, J.A., Eldeberky, Y., Won, Y., 1993. Spectral Boussinesq modelling of breaking waves. In: Magoon, O.T., Hemsley, J.M. (Eds.), In Ocean Wave Measurements and Analysis. Am. Soc. Civ. Eng., New York, pp. 813–820.

Beji, S., Battjes, J.A., 1993. Experimental investigation of wave propagation over a bar. Coastal Eng. 19, 151–162.

Beji, S., Nadaoka, K., 1996a. A formal derivation and numerical modelling of the improved Boussinesq equations for varying depth. Ocean Eng. 23 (8), 691–704.

Beji, S., Nadaoka, K., 1996b. Nonlinear refraction–diffraction of surface waves over arbitrary depths Proc. 25th Coastal Eng. Conf., pp. 1048–1059.

Beji, S., Nadaoka, K., 1997a. A time-dependent nonlinear mild-slope equation for water waves. Proc. R. Soc. Lond. A 453, 319–332.

Beji, S., Nadaoka K., 1997b. Spectral modelling of nonlinear shoaling and breaking over arbitrary depths. Proc. Coastal Dynamics '97, pp. 285–294.

Bryant, P.J., 1973. Periodic waves in shallow water. J. Fluid Mech. 59, 625–644.

Chapalain, G., Cointe, R., Temperville, A., 1992. Observed and modeled resonantly interacting progressive water-waves. Coastal Eng. 16, 267–300.

Freilich, M.H., Guza, R.T., 1984. Nonlinear effects on shoaling surface gravity waves. Phil. Trans. R. Soc. Lond. A 3, 1–41.

Madsen, P.A., Murray, R., Sørensen, O.R., 1991. A new form of the Boussinesq equations with improved linear dispersion characteristics. Coastal Eng. 15, 371–388.

Madsen, P.A., Sørensen, O.R., 1992. A new form of the Boussinesq equations with improved linear dispersion characteristics: Part 2. A slowly-varying bathymetry. Coastal Eng. 8, 183–204.

Madsen, P.A., Sørensen, O.R., 1993. Bound waves and triad interactions in shallow water. Ocean Eng. 20 (4), 359–388.

Mase, H., Kirby, J.T., 1992. Hybrid frequency-domain KdV equation for random wave transformation. Proc. 23th Coastal Eng. Conf., pp. 474–487.

Mei, C.C., 1989. The Applied Dynamics of Ocean Surface Waves, World Scientific, 740 pp.

Miles, J.W., 1980. Solitary waves. Ann. Rev. Fluid Mech. 12, 11–43.

Nadaoka, K., Beji, S., Nakagawa, Y., 1994. A fully-dispersive weakly-nonlinear wave model and its numerical solutions. Proc. 24th Coastal Eng. Conf., pp. 427–441.

Nadaoka, K., Beji, S., Nakagawa, Y., 1997. A fully dispersive weakly nonlinear model for water waves. Proc. R. Soc. Lond. A 453, 303–318.

Nakamura, S., Katoh, K., 1992. Generation of infragravity waves in breaking process of wave groups. Proc. 23th Coastal Eng. Conf., pp. 990–1003.

Nwogu, O., 1993. Alternative form of Boussinesq equations for nearshore wave propagation. J. Waterway, Port, Coastal, and Ocean Eng. 9 (6), 618–638.

Nwogu, O., Takayama, T., Ikeda, N., 1992. Numerical simulation of the shoaling of irregular waves using a new Boussinesq model. Rep. of Port and Harbour Res. Inst. 31 (2), 3–19.

Rayleigh, L., 1876. On waves. Phil. Mag. 1, 257–279.

Wiegel, R.L., 1964. Oceanographical Engineering, Prentice-Hall, 532 pp.

Witting, J.M., 1984. A unified model for the evolution of nonlinear water waves. J. Comp. Phys. 56, 203–236.